Spectroscopy of thulium-doped tantalum pentoxide waveguides on silicon

AMY S. K. TONG[#], COLIN J. MITCHELL[#], ARMEN AGHAJANI, NEIL SESSIONS, G. SENTHIL MURUGAN, JACOB I. MACKENZIE AND JAMES S. WILKINSON*

Optoelectronics Research Centre, University of Southampton, Southampton, SO17 1BJ, UK
[#]These authors contributed equally to this work
**Corresponding author: jsw@soton.ac.uk*

Abstract: The spectroscopic properties and laser operation of thulium-doped tantalum pentoxide (Tm:Ta_2O_5) waveguides are reported in this paper. Fluorescence ranging from 1600 nm to 2200 nm, corresponding to the $^3F_4 \rightarrow {}^3H_6$ transition was observed from 3 wt% Tm:Ta_2O_5 waveguides pumped at a wavelength of 795 nm. Measurements of excited-state lifetime, the emission and absorption spectra, with subsequent calculation of the cross-sections for the deposited films, reveal its potential as a gain medium. Laser operation at a wavelength of 1865 nm was obtained with feedback from the polished end faces alone, demonstrating gain of >9 dB/cm.

1. Introduction

Optical sources and amplifiers operating at wavelengths near 2 μm are important for applications from remote sensing and LIDAR [1], medical diagnostics and surgical systems [2], to free-space and optical fiber communications [3]. Thulium-doped crystals and glasses are of significant interest for these applications, potentially offering low noise, high efficiency, and high-power operation. They can be optically pumped in-band at ~1.6 μm or using a "two-for-one" cross-relaxation process by pumping at ~800 nm, where high-power low-cost semiconductor laser diodes are readily available. Tm-doped silicate glass optical fiber devices exhibit high efficiency and high power (>1 kW CW [4]) and high gain (5.8 dB/cm [5]) leading to excellent performance as individual fiber components.

In comparison with fiber devices, integrated photonics offers the potential for enhanced functionality combined with a robust construction, good thermal management, and low-cost mass-production of complex optical circuits. Glass and crystalline waveguide lasers operating at ~2 μm have been demonstrated based on various fabrication methods, for example by: ion-implantation in Tm-doped germanate glasses [6], Ti-diffusion into Tm-doped $LiNbO_3$ [7], direct bonding of Tm:YAG and sapphire [8], pulsed-laser-deposition growth of crystalline Tm:Y_2O_3 [9], and liquid-phase epitaxy in Tm-doped potassium double tungstates [9, 10]. A combination of high Tm concentration and the well-confined waveguide structure leads to a high gain coefficient as required for compact integrated devices.

In the last ten years, silicon photonics has grown to become the favored option for the wide deployment of photonic circuit technology, harnessing silicon micro/nanofabrication capabilities. However, as silicon is an indirect bandgap semiconductor it is an inefficient light emitter, leading to intensive investigation into ways to integrate laser sources and amplifiers on a silicon platform such as flip-chip bonding, transfer printing and heterogeneous epitaxy of III-V materials [11]. An alternative approach is to integrate rare-earth-doped laser sources directly in a CMOS compatible material on the silicon platform, allowing for monolithic integration and wafer scale manufacturing. Integrated rare-earth-doped lasers at wavelengths from 1 to 1.6 μm have been demonstrated on silicon with rare-earth doping using ytterbium and erbium [12, 13, 14, 15, 16]. While such systems require optical pumping with a semiconductor light source rather than the preferred electrical pumping, they have potential for high efficiency, low noise and low thermal load [13].

The presence of two-photon absorption in silicon waveguides at conventional telecoms wavelengths has led to the investigation of Si_3N_4 dielectric waveguide layers on the silicon platform to allow all-optical processing [17]. Recently a Si_3N_4 waveguide layer has been combined with a Tm-doped amorphous Al_2O_3 layer to provide gain and lasing near a wavelength of 2 μm. In particular, compact low-threshold Tm-doped microcavity lasers [18] and high-power Tm-doped DFB lasers on silicon [19] coupled to the Si_3N_4 waveguides have been demonstrated. A further recent development is the demonstration of 7.6 dB gain over a length of 6.9 cm in a Si_3N_4 waveguide overcoated with a Tm-doped TeO_2 layer [20].

Tantalum pentoxide (Ta_2O_5) is an alternative CMOS-compatible thin-film material with a higher refractive index than Si_3N_4, allowing more compact devices and flexible dispersion engineering. Ta_2O_5 also has a higher third-order nonlinearity, which can enable more efficient all-optical processes. Significantly, Ta_2O_5 is also a good host for rare-earth ions as shown for neodymium [21], erbium [15], and ytterbium [14], providing gain, which has not yet been demonstrated in Si_3N_4. Thus, Ta_2O_5 provides a route toward efficient nonlinear processing, flexible dispersion engineering, amplification and lasing, providing full circuit functionality in a *single-material* thin film. Erbium-doped alumina/silicon nitride waveguides on silicon have recently been monolithically integrated with silicon waveguides using a multilayer coupling approach [22, 23], which is also well-suited to the Tm: Ta_2O_5 waveguide system reported here.

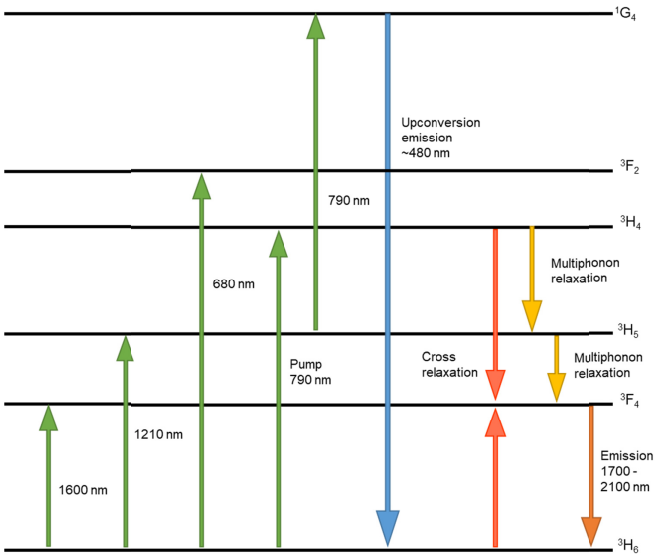

Fig. 1. Thulium ion energy level diagram.

A simplified energy level diagram for Tm^{3+} is shown in Fig. 1. By doping Ta_2O_5 with thulium-ions, emission in the range of 1400 to 2100 nm ($^3H_4 \rightarrow {}^3F_4$ and $^3F_4 \rightarrow {}^3H_6$ transitions) can be achieved by pumping at ~795 nm ($^3H_6 \rightarrow {}^3H_4$ transition). In-band pumping is also possible at ~1610 nm ($^3H_6 \rightarrow {}^3F_4$ transition) for operation on the $^3F_4 \rightarrow {}^3H_6$ transition alone. In this paper thulium-doped tantalum pentoxide (Tm:Ta_2O_5) is investigated as a gain material on silicon. While the Tm:Al_2O_3 waveguides reported in [18, 19] were pumped at 1610 nm, in this study we use a 795 nm pump, demonstrating compatibility with readily available low-cost semiconductor sources around this wavelength.

This paper presents measurements of the spectroscopic properties of thulium-doped tantalum pentoxide (Tm:Ta_2O_5) waveguides, including the $^3F_4$ excited-state lifetime, emission and absorption cross-sections around 2 μm, and the first demonstration of a Tm:Ta_2O_5 waveguide laser, compatible for integration with silicon photonics.

2. Waveguide design and fabrication

Tm-doped tantalum pentoxide waveguides on oxidized silicon wafers were designed to enable spectroscopic measurements of absorption and emission spectra, fluorescence lifetime, and conduct studies of laser operation. The fabrication was based on processes developed for Er:Ta_2O_5 waveguides on silicon [24] and ellipsometer data for refractive index from that work.

2.1 Waveguide geometry

While low-threshold lasing, and gain with low pump power, can be achieved with tightly-confined "nanowire" waveguides [25], thicker slab and rib waveguides are more appropriate for spectroscopic measurements and determination of material properties because a larger proportion of the propagating mode is confined within the core material. Slab waveguides were fabricated for fluorescence measurements, while rib waveguides were produced for absorption measurements and laser action. The slab waveguides used were 2 µm thick and had a refractive index of 2.1±0.04 at 1.55 µm. Rib waveguides for lasing were designed, using COMSOL Multiphysics, for monomode operation at a wavelength of 1.85 µm. Defining ribs in the 2-µm-thick Tm:Ta_2O_5 film, with an etch-depth of 330 nm, demonstrated that waveguides of widths less than 3 µm were found to support the fundamental mode only. The design and mode intensity profile in the TE polarization for the 3-µm-wide waveguide are shown in Fig 2. The theoretical FW1/e^2 spot size at a wavelength of 1.866 µm was 4.6 µm in the x-direction and 1.1 µm in the y-direction, and at the pump wavelength of 795 nm the spot size was 3.8 µm by 1.0 µm. Rib waveguides of 20 µm width were used for absorption measurements, ensuring strong mode confinement within the core to give an accurate measurement for the doped material only. The larger waveguide also offers reasonable input-coupling efficiency of white light from an SMF28 optical fiber.

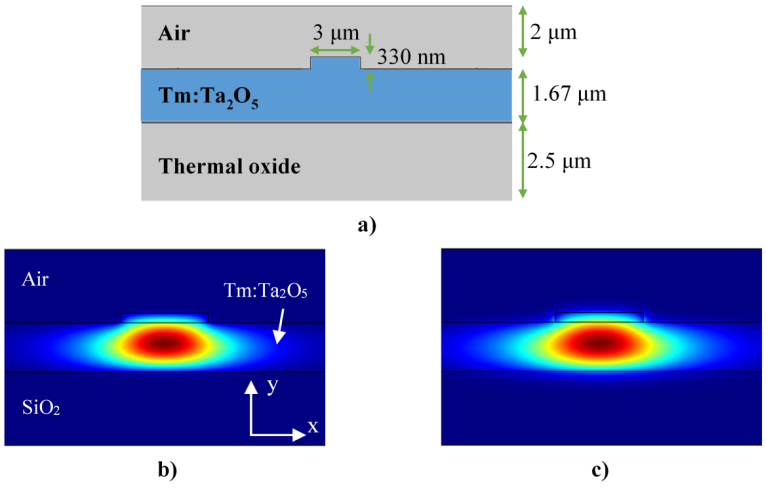

Fig. 2. 3-µm rib waveguide laser a) dimensions, and simulated mode intensity profile in TE polarization at b) 795 nm and c) 1866 nm.

2.2 Waveguide fabrication

Tm:Ta_2O_5 films, 2 µm thick, were deposited by radio-frequency (RF) sputtering on top of a 2.5-µm-thick thermal oxide layer on 4" silicon wafers. The 150mm diameter pressed ceramic sputtering target was made from powder or Ta_2O_5 with a nominal 3 wt% of Tm_2O_3. Deposition was performed at a pressure of 10 mTorr in an oxygen (5 sccm) and argon (20 sccm) atmosphere, at an RF power of 300W, resulting in a deposition rate of

~3.33 nm/min. After deposition, the wafers were annealed in an oxygen atmosphere to reduce oxygen deficiency and stress in the film. Annealing times of 2 and 12 hours with temperatures between 500°C to 650°C were used, to study the respective influence on fluorescence lifetime and intensity. The composition of the annealed films was measured using EDX to verify the Tm concentration, which was found to be $(1.1\pm0.1) \times 10^{21}$ Tm ions/cm^3.

Rib waveguides ranging from 2 to 20 µm in width were fabricated on wafers annealed at 650°C for 12 hours. The waveguides were patterned using conventional photolithography and etched to a depth of 330 nm by Ar ion-beam milling, using optimized parameters determined for Er:Ta_2O_5 waveguides [24], and then annealed in oxygen at 650°C for a further 2 hours.

The wafers were diced and the end-facets were mechanically polished to optical quality to yield chips of length 4.5 mm to 10 mm.

3. Spectroscopic properties of Tm:Ta_2O_5

In order to assess the potential of Tm:Ta_2O_5 for gain and lasing, and to provide parameters for input to simulations, accurate measurement of material properties was required. The excited-state lifetime, emission spectrum and cross-section, and the absorption spectrum and cross-section were experimentally determined for the fabricated Tm:Ta_2O_5 waveguides as described below.

3.1 Excited-state lifetime measurements

Fluorescence measurements were performed on the 2-µm-thick Tm:Ta_2O_5 slab waveguides using the apparatus shown in Fig. 3. The optimum pump wavelength had previously been determined to be 795 nm, where the highest fluorescence power was achieved [26]. Output from a Ti:sapphire laser, tuned to the pump wavelength of 795 nm, was mechanically chopped at 170 Hz and then end-fire coupled into the slab waveguide using an aspheric lens (Lens 3). Fluorescence was collected at 90° to the plane of the waveguide using a proximity-coupled fiber with a 1-mm-diameter core (Thorlabs SM2000), after which the light was collimated with an aspheric lens (Thorlabs C230TMD-C), passed through a long-pass filter to remove pump light (Schott RG1000, cut-off 1 µm), before being focused onto an InGaAs detector (DET10D/M) by a second aspheric lens (Thorlabs A260TM-C). The collected fluorescence signal was recorded on an oscilloscope and its decay after the pumping pulse is shown on a logarithmic scale in Fig. 4a.

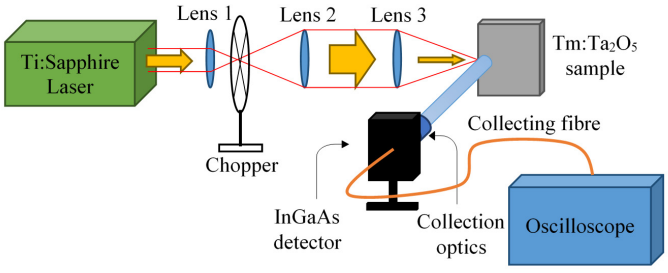

Fig. 3. Apparatus for excited-state lifetime measurements.

The effect of annealing temperature on the collected fluorescence power and excited-state lifetime were determined, as shown in Fig. 4. The highest fluorescence power and longest lifetime were attained with the sample annealed at 650°C for 12 hours. Fitting of the fluorescence decay to a single exponential yielded a lifetime of 477 ± 40 µs for this sample, with negligible residuals.

As with erbium-doped Ta_2O_5 waveguides [24], it is believed that replenishing of oxygen during annealing reduces non-radiative transitions and improves the efficiency of the emission from the excited state.

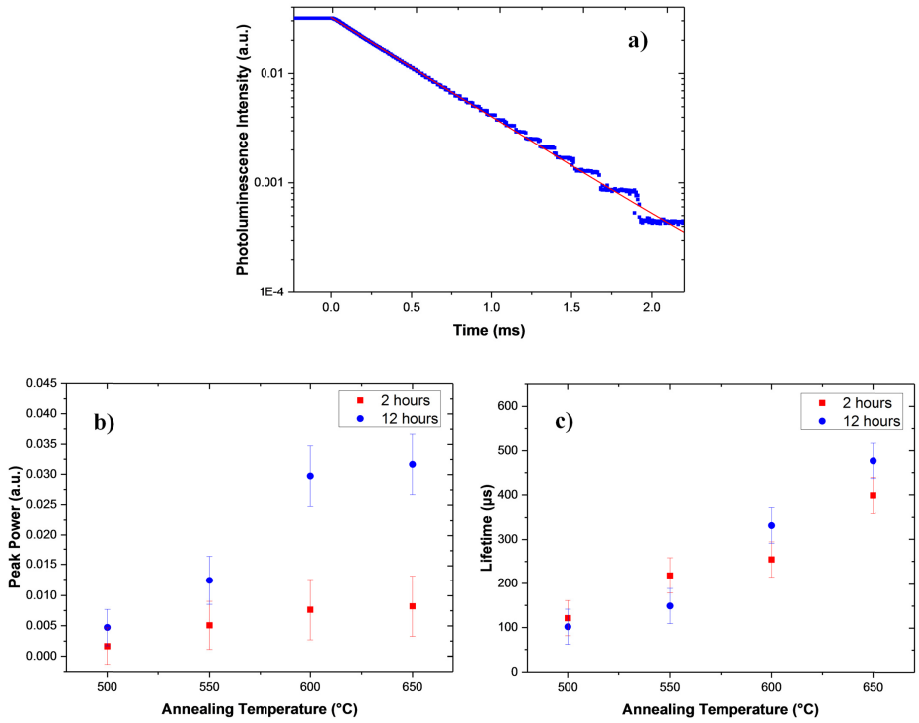

Fig. 4. a) Fluorescence decay for the sample annealed at 650°C for 12 hours, b) collected fluorescence vs. annealing temperature and time and c) $^3F_4$ excited-state lifetime vs. annealing temperature and time. All measurements used 2-µm-thick Tm:Ta_2O_5 slab waveguides.

3.2 Absorption spectrum and cross-section

Spectral absorption measurements between 600 nm and 1350 nm were performed on a 20-µm-wide rib waveguide of length 7.7 mm, fabricated using the process described in Section 2. Light from a tungsten halogen bulb coupled into a standard SMF28 fiber was butt coupled to the rib waveguide. The transmitted power was collected with a multimode fiber (Thorlabs GIF625) butted up to the output end of the waveguide and recorded with an OSA (Yokogawa AQ6370). A reference measurement was taken with the input fiber butted directly up to the collection fiber, and the transmission spectrum determined as the ratio of these two spectra. A baseline was subsequently subtracted from the transmission spectra in order to attain the final data. This baseline was calculated by fitting a second order polynomial to regions of the spectra assumed to have zero absorption away from the observed peaks. In this way, background waveguide effects such as facet reflections and broadband waveguide loss not arising from the Tm ions were eliminated from the transmission spectra, yielding the absorption due to the Tm ions alone.

The absorption cross-section was calculated from the transmission spectrum using the Beer-Lambert law and the measured length and Tm concentration, and is shown in Fig. 5a. The peak absorption cross-section in the pump waveband, corresponding to the $^3H_6 \rightarrow {}^3H_4$ transition, was $(5.0\pm0.6) \times 10^{-21}$ cm^2 at 792 nm. Other absorption peaks were observed at around 685 nm and 1210 nm corresponding to the $^3H_6 \rightarrow {}^3F_2$ and $^3H_6 \rightarrow {}^3H_5$ transitions, respectively. The uncertainties in the cross-sections were estimated by combining the (dominant) uncertainty in the measured density of Tm ions in the tantalum pentoxide films with estimates of the uncertainty in the absorption and fluorescence measurements.

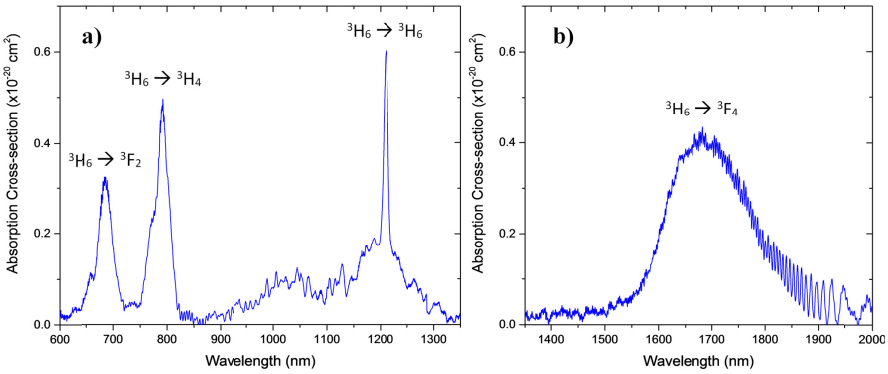

Fig. 5. Absorption cross-section spectra of Tm^{3+}:Ta_2O_5 for a) short wavelength, and b) long wavelength regions.

Spectral absorption measurements at wavelengths between 1.3 µm and 2 µm were performed on a 20-µm-wide rib waveguide of length 4.5 mm using the same procedure, but replacing the Yokogawa OSA and SMF28 input fiber with a Thorlabs OSA (OSA203C) and SMF28e input fiber suitable for the longer wavelengths. The calculated peak absorption cross-section was found to be $(4.1\pm0.4) \times 10^{-21}$ cm^2 at a wavelength of 1682 nm (Fig. 5b). Fluctuations on the long-wavelength side of the spectra in Fig. 5b is believed to be an artefact of modal interference within the broad multimode waveguide.

3.3 Emission spectrum and cross-section

The emission spectrum was measured using the same apparatus as that employed for the lifetime measurements (Fig. 3), except that the detector and oscilloscope were replaced by the long wavelength OSA. A broad emission peak ranging between 1.6 and 2.1 µm was observed, corresponding to the $^3F_4 \rightarrow {}^3H_6$ transition (Fig. 6a). A second peak in the region of 1475 nm was also observed, and this peak is attributed to the optical transition from the upper pump state ($^3H_4 \rightarrow {}^3F_4$).

The emission cross-section for the $^3F_4 \rightarrow {}^3H_6$ transition is shown in Fig. 6b and was calculated from the fluorescence spectrum and the measured lifetime using the Füchtbauer-Ladenburg (FL) method [27], scaled by the quantum efficiency (QE). Fluorescence below 1570 nm and above 2300 nm was excluded in the calculation as not originating from the $^3F_4$ level. To determine the QE both the absorption cross section and unscaled FL emission cross-section spectra were transformed using McCumber/reciprocity analysis [28] then compared. It was assumed that the ratio of the partition functions for the respective energy levels is 1 as this is a typical value obtained for Tm-doped gain media. A second unknown variable, the zero-phonon line (ZPL) wavelength, also needs to be identified to enable this analysis. Consequently, with two unknowns and two independent spectra, the final emission cross section could be determined. In adjusting the values for QE and ZPL a match for the short-wavelength rising edge of the absorption cross-section spectra and long-wavelength falling edge of the emission cross-section spectra were used, as the regions of strongest signals in the respective data. As such, the respective values for QE and ZPL were estimated to be 0.2 and 1739 nm. From this method we estimate the *radiative* lifetime to be 2.4 ms. The peak emission cross-section for this transition was found to be $(5.7\pm0.7) \times 10^{-21}$ cm^2 at a wavelength of 1772 nm. Sharp spectral artefacts are observed in the emission spectrum at wavelengths around 1.9 µm and these are believed to be due to residual atmospheric absorption in the light path between the waveguide and OSA detector array.

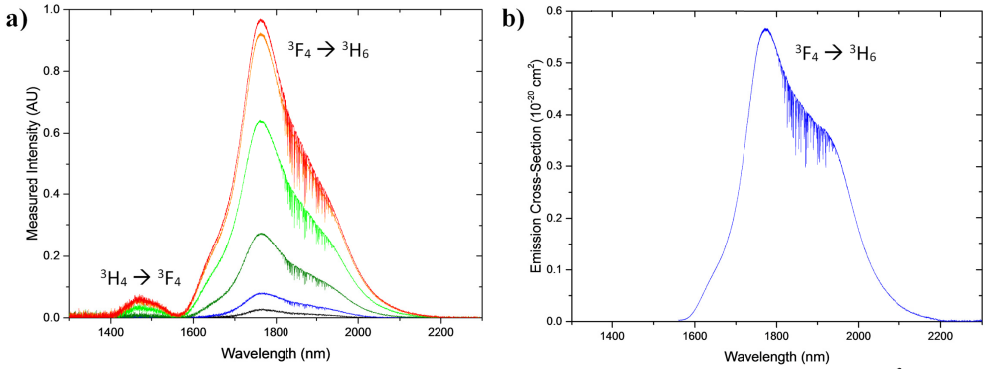

Fig. 6. Emission spectra a) fluorescence with increasing pump power, b) emission cross-section for Tm^{3+}:Ta_2O_5 between for the $^3F_4 \rightarrow {}^3H_6$ transition with a quantum efficiency of 0.2.

4. Tm:Ta_2O_5 Waveguide Laser

In order to study the potential for lasing, a 3-μm-wide and 1-cm-long Tm:Ta_2O_5 rib waveguide was end-fire pumped at a wavelength of 795 nm, with the Fabry-Perot cavity formed by the polished waveguide end facets alone (11.6% reflectivity). The apparatus used is shown in Fig. 7. Light from a Ti:sapphire laser was focused into a HI1060 fiber (Corning) using an aspheric lens, to provide a near-Gaussian beam. The output of the fiber was collimated and focused into the waveguide end using another aspheric lens. The waveguide output signal was passed through a further aspheric lens and a long-pass filter (Semrock LP02-980RU-25) to minimize the transmission of any light at the pump wavelength, and then coupled into an OSA to measure the output spectrum.

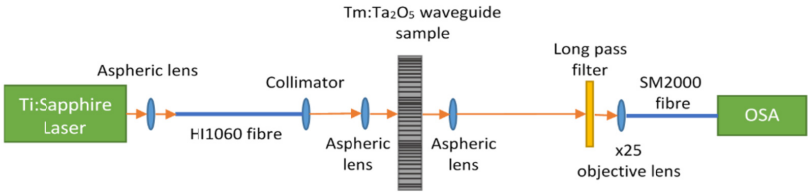

Fig. 7. Apparatus for characterizing lasing in a Tm:Ta_2O_5 waveguide

At an *incident* pump power of 170 mW, corresponding to a *launched* pump power of ~44 mW calculated from the overlap of the modal field and the incident beam, sharp emission peaks were observed at 1238 nm and 1855/1858 nm, corresponding to $^3H_5 \rightarrow {}^3H_6$ and $^3F_4 \rightarrow {}^3H_6$ transitions respectively, as shown in Fig. 8, and demonstrating the onset of lasing. Er-doped Ta_2O_5 waveguides have exhibited propagation losses of 0.65 ± 0.05 dB at a wavelength of 1600nm [15] and we expect a similar loss for these Tm-doped waveguides at wavelengths near 1.8 μm. The cavity round trip loss was estimated to be ~20dB, including (i) transmission through two end facets of 9 dB each, due to reflection solely depending on Fresnel reflection, and (ii) combined propagation losses and reabsorption losses, from residual Tm^{3+} ions in the ground-state, of approximately 1 dB each way. The calculated launched pump power threshold for lasing at 1858 nm was estimated to be ~15 mW using conventional theory for waveguide lasers with reabsorption [29], and the lifetime, quantum efficiency, cross-sections at 1858 nm and mode sizes estimated above.

The discrepancy between the measured and calculated pump power threshold may be due to a combination of excess loss at the end-facets, non-ideal pump/waveguide alignment, operation of the laser far from the low ground-state depletion regime assumed in so that much of the launched pump power is not absorbed, non-unity pump input coupling efficiency, and phenomena such as energy transfer upconversion (ETU). Further studies at lower

concentration and with improved laser cavity configurations are underway. However, this preliminary demonstration shows that a gain of at least 9 dB/cm is achievable in the waveguide films produced with our nominally 3 wt% Tm_2O_3 doped Ta_2O_5 target.

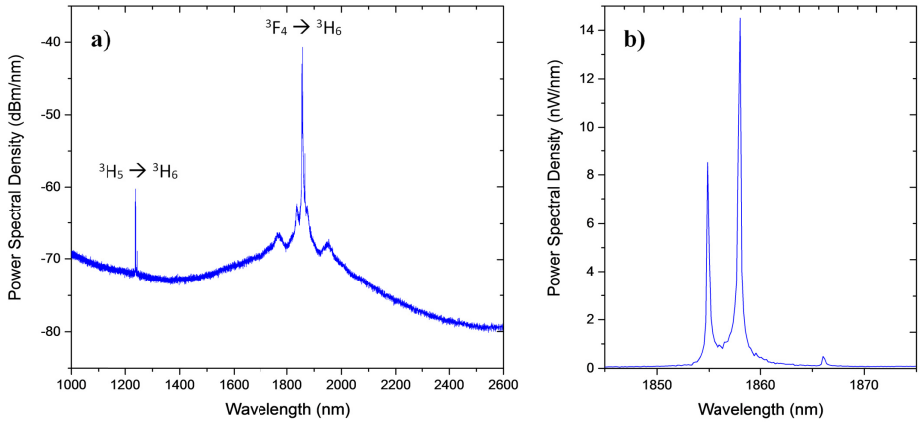

Fig. 8. Laser output spectrum with an incident pump power of 170 mW a) showing lasing at 1238 nm and 1858 nm, and b) expanded to show detail, on a linear scale, near 1858 nm

5. Discussion

Fluorescence from Tm:Ta_2O_5 at around 800 [30], 650, 1250 and 1550 nm [31] has been observed previously. However, the excited-state lifetimes and absorption and emission cross-sections have not been reported, and nor has emission around 1800 nm.

Absorption and emission cross-sections. Previously reported absorption cross-sections for thulium-doped materials have been predominantly from thulium-doped silica fibers and bulk glasses. The peak absorption cross-section for the $^3H_6 \rightarrow {}^3F_4$ transition near 1.7 μm of 4.2×10^{-21} cm^2 measured in the present work is similar to that for silica fibers of 4.2×10^{-21} cm^2 [5] and Al_2O_3 thin films of 2.8×10^{-21} cm^2 [32]. The absorption cross-section for the $^3H_6 \rightarrow {}^3H_4$ transition near 790 nm in a silica fiber, reported in [33], is also similar to the absorption cross section we report here. The Tm:Ta_2O_5 emission cross-section of 5.7×10^{-21} cm^2 is slightly higher than a similarly doped silica fiber of 3.6×10^{-21} cm^2 [5], and a Tm^{3+}-doped aluminum oxide film, which was shown to have an emission cross-section of 4.7×10^{-21} cm^2 [32], as may be expected from a higher-index material.

Lifetimes. The measured excited-state lifetime of Tm:Ta_2O_5 is in a similar range to that reported for Tm-doped silica fibers with similar dopant concentrations [5]. A shorter lifetime of 250 μs [34] was observed from a high-index nanoparticulate silicon film, but a longer lifetime of 2.32 ms was observed in Al_2O_3 [32] and other lower dopant concentration silica fibers [35]. Although the excited-state lifetime is expected to be shorter in a higher index material, the quantum efficiency of 0.2 implies that the measured lifetime is significantly shortened by non-radiative processes, and the radiative lifetime is estimated to be 2.4 ms.

Gain. The emission and absorption cross-sections deduced here show that a Tm:Ta_2O_5 waveguide with a Tm dopant concentration of 1.1×10^{21} ions/cm^3 should yield a gain of ~15 dB/cm at a wavelength of 1858 nm with 80% of the Tm^{3+} ions pumped into the $^3F_4$ energy level, assuming zero propagation loss and neglecting ETU, which will clearly have an impact as observed in Er-doped Al_2O_3 waveguides [36]. The preliminary lasing results show that a gain of at least 9 dB/cm has been achieved at 1238 nm, 1855 nm and 1858 nm, higher than that achieved with similar concentration of thulium doping in silica fibers [5], and clamped by the cavity loss. Significantly more gain is likely available, and this is presently under investigation.

6. Conclusion

The spectroscopic characteristics of Tm:Ta_2O_5 waveguides on silicon were investigated in this paper. A broad emission from 1450 to 2100 nm was observed when pumped at 795 nm and the corresponding excited-state lifetime was measured to be (477±40) μs. The absorption spectrum of Tm:Ta_2O_5 from 600 to 2000 nm was measured, and the peak absorption cross-section at 792 nm was found to be $(5.0\pm0.6) \times 10^{-21}$ cm^2 and at 1682 nm it was $(4.1\pm0.4) \times 10^{-21}$ cm^2. The peak emission cross-section was found to be $(5.7\pm0.7) \times 10^{-21}$ cm^2 at 1772 nm, significantly higher than silicate glasses. The potential as a laser material was evaluated by pumping the waveguides at 795 nm and achieving lasing from the Fresnel reflection of the polished end facets alone. These results confirm that a gain of at least 9 dB/cm has been achieved. While low pump power threshold and high slope efficiency for efficient operation will require further optimization of the materials and waveguide properties including background loss and Tm concentration, and an optimized laser cavity. Tm:Ta_2O_5 is a promising material for realizing integrated lasers and amplifiers compatible with silicon photonics.

Funding

This work was supported by the UK EPSRC Programme Grant, Silicon Photonics for Future Systems EP/L00044X/1, by Amy Tong's EPSRC studentship 1513767, and for J. I. Mackenzie by EP/N018281/1 and EP/P027644/1.

Disclosures

The authors declare no conflicts of interest.

Open Access Statement

All data supporting this study are openly available from the University of Southampton repository at https://doi.org/10.5258/SOTON/D1371

References

1. Q. Wang, J. Geng and S. Jiang, "2-μm Fiber Laser Sources for Sensing," Optical Engineering, vol. 53, no. 6, p. 061609, 2013.
2. Y. Barbalat, M. C. Velez, C. I. Sayegh and D. E. Chung, "Evidence of the Efficacy and Safety of the Thulium Laser in the Treatment of Men with Benign Prostatic Obstruction," Therapeutic Advances in Urology, vol. 8, no. 3, pp. 181-191, 2016.
3. F. G. Gunning, N. Kavanagh, E. Russell, R. Sheehan, J. O'Callaghan and B. Corbett, "Key Enabling Technologies for Optical Communications at 2000 nm," Appl. Optics, vol. 57, no. 22, pp. E64-E70, 2018.
4. P. F. Moulton, G. A. Rines, E. V. Slobodtchikov, K. F. Wall, G. Frith, B. Samson and A. L. Carter, "Tm-doped Fiber Lasers: Fundamentals and Power Scaling," IEEE Journal of Selected Topics in Quantum Electronics, vol. 15, no. 1, pp. 85-92, 2009.
5. Y.-W. Lee, H.-Y. Ling, Y.-H. Lin and S. Jiang, "Heavily Tm^{3+}-doped Silicate Fiber with High Gain per Unit Length," Optical Materials Express, vol. 5, no. 3, pp. 549-557, 2015.
6. D. P. Shepherd, D. J. B. Brinck, J. Wang, A. C. Tropper, D. C. Hanna, G. Kakarantzas and P. D. Townsend, "1.9 μm Operation of a Tm: lead Germanate Glass Waveguide Laser," Optics Lett., vol. 19, no. 13, pp. 954-956, 1994.
7. J. P. De Sandro, J. K. Jones, D. P. Shepherd, M. Hempstead, J. Wang and A. C. Tropper, "Non-photorefractive CW Tm-indiffused Ti:$LiNbO_3$ Waveguide Laser Operating at Room Temperature," IEEE Photonics Technology Letters, vol. 8, no. 2, pp. 209-211, 1996.
8. J. I. Mackenzie, S. C. Mitchell and R. M. H. a. S. D. Beach, "15 W Diode-side-pumped Tm:YAG Waveguide Laser at 2 μm," Electron. Lett., vol. 37, no. 14, p. Electronics Letter, 2001.
9. J. W. Szela, K. A. Sloyan, T. L. Parsonage, J. I. Mackenzie and R. W. Eason, "Laser Operation of a Tm:Y_2O_3 Planar Waveguide," Optics Express, vol. 21, no. 10, pp. 12460-12468, 2013.
10. J. J. Carvajal, W. Bolaños, X. Mateos, F. Díaz and M. Aguiló, "Tm^{3+}-based Waveguide Lasers in Monoclinic Double Tungstates," Journal of Luminescence, vol. 133, pp. 262-267, 2013.
11. Z. Wang, A. Abbasi, U. Dave, A. De Groote, S. Kumari, B. Kunert, C. Merckling, M. Pantouvaki, Y. Shi, B. Tian, K. Van Gasse, J. Verbist, R. Wang, W. Xie, J. Zhang, Y. Zhu, J. Bauwelinck, X. Yin, Z. Hens, J. Van Campenhout and et al., "Novel Light Source Integration Approaches for Silicon Photonics," Laser & Photonics Reviews, vol. 11, no. 4, p. 1700063, 2017.

12. J. D. Bradley, E. S. Hosseini, Purnawirman, Z. Su, T. N. Adam, G. Leake, D. Coolbaugh and M. R. Watts, "Monolithic Erbium- and Ytterbium-doped Microring Lasers on Silicon Chips," Optics Express, vol. 22, no. 10, pp. 12226-12237, 2014.
13. M. Belt and D. J. Blumenthal, "Erbium-doped Waveguide DBR and DFB Laser Arrays Integrated Within an Ultra-low-loss Si_3N_4 Platform," Optics Express, vol. 22, no. 9, pp. 10655-10660, 2014.
14. A. Aghajani, G. S. Murugan, N. P. Sessions, V. Apostolopoulos and J. S. Wilkinson, "Waveguide Lasers in Ytterbium-doped Tantalum Pentoxide on Silicon," Optics Lett., vol. 40, no. 11, pp. 2549-2552, 2015 .
15. A. Z. Subramanian, G. S. Murugan, M. N. Zervas and J. S. Wilkinson, "Spectroscopy, Modeling, and Performance of Erbium-Doped Ta_2O_5 Waveguide Amplifiers," Journal of Lightwave Technology, vol. 30, no. 10, pp. 1455-1462, 2012.
16. E. H. Bernhardi, H. A. van Wolferen, K. Wörhoff, R. M. De Ridder and M. Pollnau, "Highly Efficient, Low-threshold Monolithic Distributed-Bragg-reflector Channel Waveguide Laser in Al_2O_3:Yb^{3+}," Optics Lett., vol. 36, no. 5, pp. 603-605, 2011.
17. D. J. Moss, R. Morandotti, A. L. Gaeta and M. Lipson, "New CMOS-compatible Platforms Based on Silicon Nitride and Hydex for Nonlinear Optics," Nature Photonics, vol. 7, no. 8, p. 597, 2013.
18. Z. Su, N. Li, E. S. Magden, M. Byrd, T. N. Adam, G. Leake, D. Coolbaugh, J. D. Bradley and M. R. Watts, "Ultra-compact and Low-threshold Thulium Microcavity Laser Monolithically Integrated on Silicon," Optics Lett., vol. 41, no. 24, pp. 5708-5711, 2016.
19. N. Li, P. Purnawirman, Z. Su, E. S. Magden, P. T. Callahan, K. Shtyrkova, M. Xin, A. Ruocco, C. Baiocco, E. P. Ippen and F. X. Kärtner, "High-power Thulium Lasers on a Silicon Photonics Platform," Optics Lett., vol. 42, no. 6, pp. 1181-1184, 2017.
20. K. Miarabbas Kiani, H. C. Frankis, H. M. Mbonde, R. Mateman, A. Leinse, A. P. Knights and J. D. Bradley, "Thulium-doped Tellurium Oxide Waveguide Amplifier with 7.6 dB Net Gain on a Silicon Nitride Chip," Optics Lett., vol. 44, no. 23, pp. 5788-5791, 2019.
21. B. Unal, M. C. Netti, M. A. Hassan, P. J. Ayliffe, M. D. B. Charlton, F. Lahoz, N. Perney, D. P. Shepherd, C.-Y. Tai, J. S. Wilkinson and G. J. Parker, "Neodymium-doped Tantalum Pentoxide Waveguide Lasers," IEEE J. Quantum Electron., vol. 41, no. 12, pp. 1565-1573, 2005.
22. N. Li, M. Xin, Z. Su, E. Salih Magden, N. Singh, J. Notaros, E. Timurdogan, P. Purnawirman, J. D. B. Bradley and M. Watts, "A Silicon Photonic Data Link with a Monolithic Erbium-Doped Laser," Scientific Reports, vol. 10, no. 1114, 2020.
23. J. Notaros, N. Li, C. V. Poulton, Z. Su, M. J. Byrd, E. Salih Magden, E. Timurdogan, C. Baiocco, N. M. Fahrenkopf and M. Watts, ""CMOS-Compatible Optical Phased Array Powered by a Monolithically-Integrated Erbium Laser," Journal of Lightwave Technology, vol. 37, no. 24, pp. 5982-5987, 2019.
24. A. Z. Subramanian, C. J. Oton, J. S. Wilkinson and R. Greef, "Waveguiding and Photoluminescence in Er^{3+}-doped Ta_2O_5 Planar Waveguides," Journal of Luminescence, vol. 129, no. 8, pp. 812-816, 2009.
25. X. Yan, "Ytterbium Doped Tantalum Pentoxide Nanowire Waveguide Lasers," PhD Thesis, Electronics and Computer Science, University of Southampton, Southampton, United Kingdom, 2017.
26. A. S. K. Tong, C. J. Mitchell, J. I. Mackenzie and J. S. Wilkinson, "Photoluminescence of Tm-doped Ta_2O_5 Waveguides," in Proceedings of Conference on Lasers and Electro-Optics Pacific Rim (CLEO-PR), Singapore, 2017.
27. P. Loiko, S. J. Yoon, J. M. Serres, X. Mateos, S. J. Beecher, R. B. Birch, V. G. Savitski, A. J. Kemp, K. Yumashev, U. Griebner and V. Petrov, "Temperature-dependent Spectroscopy and Microchip Laser Operation of Nd:$KGd(WO_4)_2$," Optical Materials, vol. 58, pp. 365-372, 2016.
28. S. A. Payne, L. L. Chase, L. K. Smith, W. L. Kway and W. F. Krupke, "Infrared Cross-section Measurements for Crystals Doped with Er^{3+}, Tm^{3+}, and Ho^{3+}," IEEE J. Quantum Electron., vol. 28, no. 11, pp. 2619-2630, 1992.
29. W. P. Risk, "Modeling of Longitudinally Pumped Solid-State Lasers Exhibiting Reabsorption Losses," JOSA B, vol. 5, no. 7, pp. 1412-1423, 1988.
30. K. Miura, T. Osawa, Y. Yokota, T. Suzuki and O. Hanaizumi, "Fabrication of Tm-doped Ta_2O_5 Thin Films using a Co-sputtering Method," Results in Physics, vol. 4, pp. 148-149, 2014.
31. M. Macatrao, M. Peres, C. P. L. Rubinger, M. J. Soares, L. C. Costa, F. M. Costa, T. Monteiro, N. Franco, E. Alves, B. Z. Saggioro and M. R. Andreeta, "Structural and Optical Properties on Thulium-doped LHPG-grown Ta_2O_5 Fibres," Microelectronics Journal, vol. 40, no. 2, pp. 309-312, 2009.
32. P. Loiko and M. Pollnau, "Stochastic Model of Energy-transfer Processes among Rare-earth Ions. Example of Al_2O_3:Tm^{3+}," J. Phys. Chem. C, vol. 120, no. 46, pp. 26480-26489, 2016.
33. B. R. Johnson, D. J. Creeden and S. D. Setzler, "Extreme Temperature Operation of Thulium-doped Silica Fiber Lasers," Fiber Lasers XIV: Technology and Systems, vol. 10083, p. 100830J, 2017.
34. M. Murray, T. Toney Fernandez, B. Richards, G. Jose and A. Jha, "Tm^{3+} doped Silicon Thin Film and Waveguides for Mid-infrared Sources," Appl. Phys. Lett., vol. 101, no. 14, p. 141107, 2012.
35. S. D. Agger and J. H. Povlsen, "Emission and Absorption Cross Section of Thulium Doped Silica Fibers," Optics Express, vol. 14, no. 1, pp. 50-57, 2006.
36. L. Agazzi, K. Worhoff and M. Pollnau, "Energy-Transfer-Upconversion Models, Their Applicability and Breakdown in the Presence of Spectroscopically Distinct Ion Classes: A Case Study in Amorphous Al_2O_3:Er^{3+}," J. Phys. Chem. C, vol. 117, no. 13, pp. 6759-6776, 2013.